Hindawi
Science and Technology of Nuclear Installations
Volume 2021, Article ID 2420526, 6 pages
https://doi.org/10.1155/2021/2420526

Research Article

Failure Fraction Calculation of the TRISO-Coated Particle Using X-Ray Computed Tomography

Libing Zhu, Jianxun Zhao, Xincheng Xiang, Yu Zhou, and Xiangang Wang

Institute of Nuclear and New Energy Technology, Collaborative Innovation Center of Advanced Nuclear Energy Technology, Key Laboratory of Advanced Reactor Engineering and Safety, Tsinghua University, Ministry of Education, Beijing 100084, China

Correspondence should be addressed to Xiangang Wang; wangxiangang@tsinghua.edu.cn

Received 28 April 2021; Accepted 30 August 2021; Published 21 September 2021

Academic Editor: Jariah Mohamad Juoi

The geometrical shape of the TRISO-coated particle is closely related to its performance and safety. In this paper, models were set up to study the failure fraction of TRISO particle, considering the real asphericity induced by manufacturing uncertainties. TRISO is simplified as a pressure vessel model, and micro X-ray CT was employed to detect the real geometrical shape. Key geometrical parameters, thickness and volume of the real particle, were then obtained with the 3D measurement method and input into PANAMA code (a German code for fuel performance simulation). Release fraction of fission gas and failure fraction of the TRISO-coated particle were revised with the aforementioned parameters with more accuracy and compared with those of the spherical particle. Obvious increment of failure fraction of the particle is found, which may contribute to the release of fission products.

1. Introduction

Tri-structural isotropic (TRISO) particle is the core fuel form for the Generation-IV, high temperature gas-cooled reactor as well as very high temperature reactor, molten salt reactor, and gas-cooled fast reactor due to its ability to retain fission product during severe accident condition at temperature up to 1600°C. It is composed of four layers encasing a kernel, namely, porous carbon (buffer) layer, inner high-density pyrolytic carbon (IPyC) layer, silicon carbide (SiC) layer, and outer high-density pyrolytic carbon (OPyC) layer, as shown in Figure 1. One fuel pebble consists of ~12,000 particles.

PANAMA is a German model built to study the behavior and performance of fuel element. TRISO-coated particle is simplified as a pressure vessel (PV) model, only considering the SiC layer because the SiC layer is the main stress holder and fission gas retention barrier. If the stress of the SiC layer exceeds the tensile strength of it, the pressure vessel will fail. The PANAMA model calculates failure fraction for a pressure vessel of a particle with complete consideration of fission product behavior. Thus, the PV model is used to calculate failure fraction of the particle in this paper.

Several models have been proposed to study the TRISO particle, but most of them assume that the particle has an ideal sphericity without considering manufacturing uncertainties. Moreover, failure fraction calculation based on the pressure vessel model is directly dependent on the geometrical shape of the particle. Fission product-induced inner pressure is proportional to the volume of UO_2 kernel and the thickness of the buffer layer. The thickness of the SiC layer has something to do with thermal composition rate and erosion-induced thinning rate. The PARFUME model studied the failure fraction of a particle as a function of asphericity [1–3] and simulated stress distribution of the SiC layer with corrosion holes [4]. Cao et al. [5] and Liu et al. [6] did research about the effect of asphericity on SiC layer stress. But they just changed the shape of the TRISO particle manually. Bari et al. [7] measured the void volume of OPyC of surrogate TRISO by reconstructing a 3D volume rendering of the particle using CT slices and calculated thermal diffusivity with the finite element method. Lowe et al. [8] measured detailed pore sizes, distribution, and interconnectivity with multiscale X-ray CT. However, the effect of the real thickness and volume of the particle on the

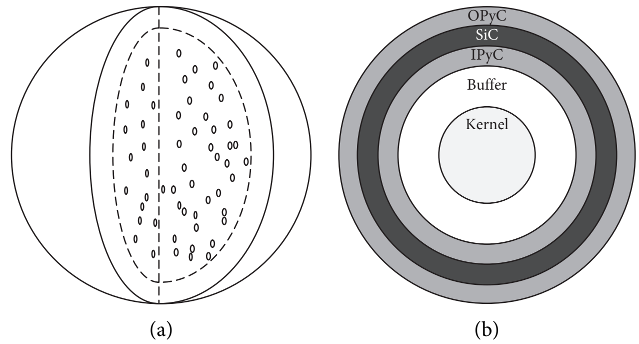

Figure 1: (a) Scheme of fuel pebble and (b) TRISO-coated particle.

failure fraction of the pressure vessel model was not addressed. Thus, an improved pressure vessel model is proposed. The real geometrical parameters with 3D measurement using micro-CT are used to study the sensitivity of failure fraction to them. Measured thickness and volume of the particle are input into PANAMA code to obtain more accurate failure fraction.

2. Materials and Methods

2.1. Pressure Vessel Model. The following equation deduction of PANAMA shows the theoretical relationship between failure fraction and geometrical parameters used in this paper, reproduced from references [9, 10].

The TRISO-coated particle is simplified to a pressure vessel model only considering the SiC layer. Failure fraction is a function of stress, σ_t, tensile strength, σ_0, and Weibull parameter, m, as shown in equation (1). The SiC layer is assumed to be a "thin wall." Equation (2) represents a simplified stress calculation.

$$\Phi(t,T) = 1 - \exp\left\{-\ln 2\left(\frac{\sigma_t}{\sigma_0}\right)^m\right\}, \tag{1}$$

$$\sigma_t = \frac{rp}{2d_0}, \tag{2}$$

where r is the mean radius of the SiC layer (m); p is the gas pressure (Pa); and d is the initial thickness of the SiC layer (m).

Inner pressure is directly dependent on the release fraction of fission gases, the void volume, and the kernel volume. Release fraction of fission gas is also related to the kernel volume, surface area, and radius which are measured by CT accurately in this paper.

2.1.1. Pressure Vessel Model including Corrosion. Φ_p is failure fraction based on a pressure vessel model and includes fission product corrosion on the SiC layer which is significant below 2000°C. Failure fraction is shown in equation (3). The thinning rate of the SiC layer under fission product corrosion is shown in equation (4) [11].

$$\Phi_p(t,T) = 1 - \exp\left\{-\ln 2\left(\frac{\sigma_t}{\sigma_0}\right)^m\right\}. \tag{3}$$

SiC stress:

$$\sigma_t = \frac{rp}{2d} = \frac{rp}{2d_0}\left(\frac{(1+\dot{v}t)}{d_0}\right), \tag{4}$$

where $\dot{v}$ is the volume corrosion rate [12]; r is the mean radius of the SiC layer (m); and d is the thickness of the SiC layer after corrosion (m).

2.1.2. Pressure Vessel Model including Thermal Decomposition. Φ_d is the failure fraction induced by thermal decomposition, which is dominant beyond 2000°C. Failure fraction is dependent on the thinning rate and inversely proportional to initial thickness of the SiC layer.

$$\Phi_d(t,T) = 1 - \exp\left\{-\alpha\xi^{\beta}\right\}, \tag{5}$$

where α and β are constants and can be derived from German experimental data [9] and ξ is the action integral which is integration of thinning rate function.

2.1.3. Overall Failure Fraction. The overall failure fraction is a function of failure fraction including corrosion and thermal decomposition as shown in the following equation:

$$\Phi_{\text{total}} = 1 - \left(1 - \Phi_p\right)\left(1 - \Phi_d\right). \tag{6}$$

2.2. Experiment. In our previous study, synchrotron phase-contrast CT and Xradia microXCT 400 were used to acquire slices of the surrogate TRISO-coated particle for three-dimensional measurement. A single TRISO-coated particle was scanned using Xradia microXCT 400. Source-to-object distance (SOD) was 37 mm, and object-to-detector distance (ODD) was 8 mm. Voxels are 1.12 μm. The specimen was rotated over 360°, and 833 slices were collected. Acquisition time was 18 s. Another particle was scanned with in-line X-ray synchrotron phase-contrast CT. ODD was 30 mm, and photon energy was 50 keV. Pixel pitch was 0.65 μm. The phase-attenuation duality Paganin algorithm (PAD-PA) was used for phase retrieval. CT slices were reconstructed by the filtered back-projection method with 727 projections [13, 14]. Figures 2(a) and 2(b) demonstrate the slices obtained with phase-contrast CT and micro-CT.

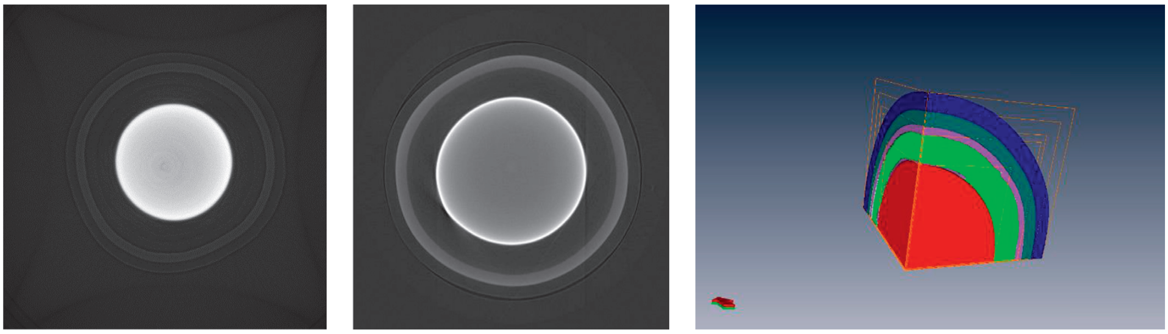

(a) (b) (c)

Figure 2: (a) Synchrotron phase-contrast CT slice. (b) Micro-CT slice. (c) A quarter cut of 3D volume rendering of the particle.

Table 1: Measured geometrical parameters with CT.

	Xradia micro-CT Mean thickness (μm)	Phase-contrast CT Mean thickness (μm)	Ideal TRISO Design thickness (μm)
Kernel	269.64	243.96	250
Buffer	67.45	79.49	95
IPyC	21.35	50.60	40
SiC	39.83	33.83	35
OPyC	45.80	41.65	40

Table 2: Non-geometrical input parameters for failure fraction calculation.

Attribute	Units	Value
Heavy metal burnup	%FIMA	9
Irradiation time	Day	1401.60
Irradiation time being read	Hour	180
Number of time steps		12
Time step length	Hour	1
Time-temperature history	°C	760 (initial step) 1122 (end step)
Average irradiation temperature	°C	813.68
Number of oxygen atoms per fission before heating		0.01838
Fast neutron fluence	10^{25} n/m^2	1.27
SiC strength	MPa	834.00 (before irradiation) 759.61 (after irradiation)
Weibull parameter		8.02 (before irradiation) 6.98 (after irradiation)

Amira is a 3D data visualization, analysis, and modelling system [15]. The slices were imported into Amira 5.4.3 to reconstruct 3D volume rendering of the particle for three-dimensional measurement as shown in Figure 2(c). The thickness and volume of kernel and coating layers were obtained as shown in Table 1. The real TRISO is aspherical while the shape of it is still similar to sphericity, so the mean radii of all layers, set integer firstly, are input into PANAMA to revise the failure fraction of the pressure vessel model.

2.3. Failure Fraction Calculation. The basic irradiation conditions and nominal material properties used in this method are summarized in Table 2 [9]. These non-geometrical parameters are kept the same and constant in PANAMA code for two kinds of TRISO model.

3. Results

As discussed in Section 2, fission gas release contributes mainly to pressure vessel failure, so fission gas release fraction as a function of irradiation time is first plotted and illustrated in Figure 3. Figures 4–6 show the failure fraction including corrosion, failure fraction including thermal decomposition, and overall failure fraction as a function of irradiation time. The signs GAS.REF, PHI1, PHI2, and PHI represent gas release fraction, failure fraction including corrosion, failure fraction including thermal decomposition,

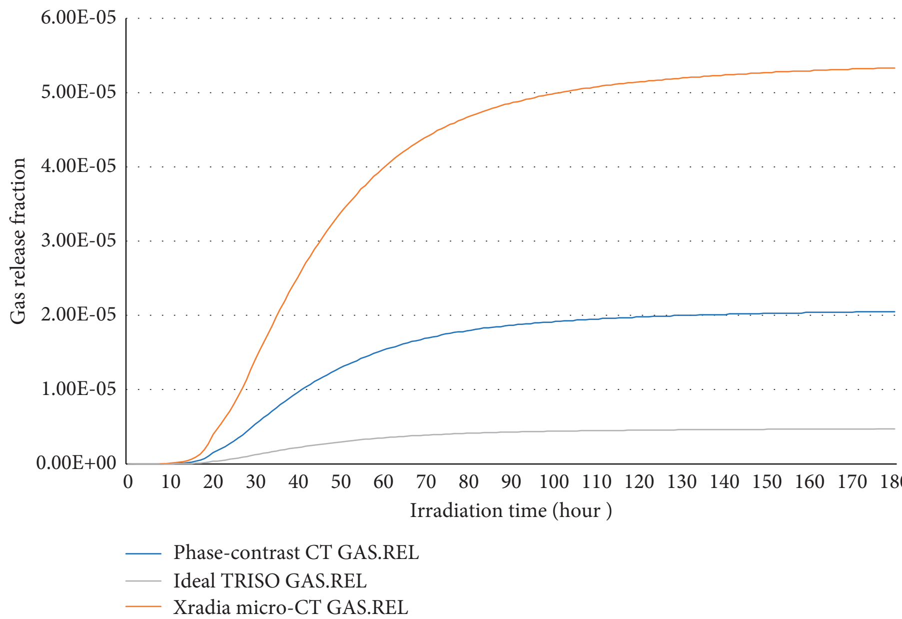

FIGURE 3: Release fraction of fission gas versus irradiation time.

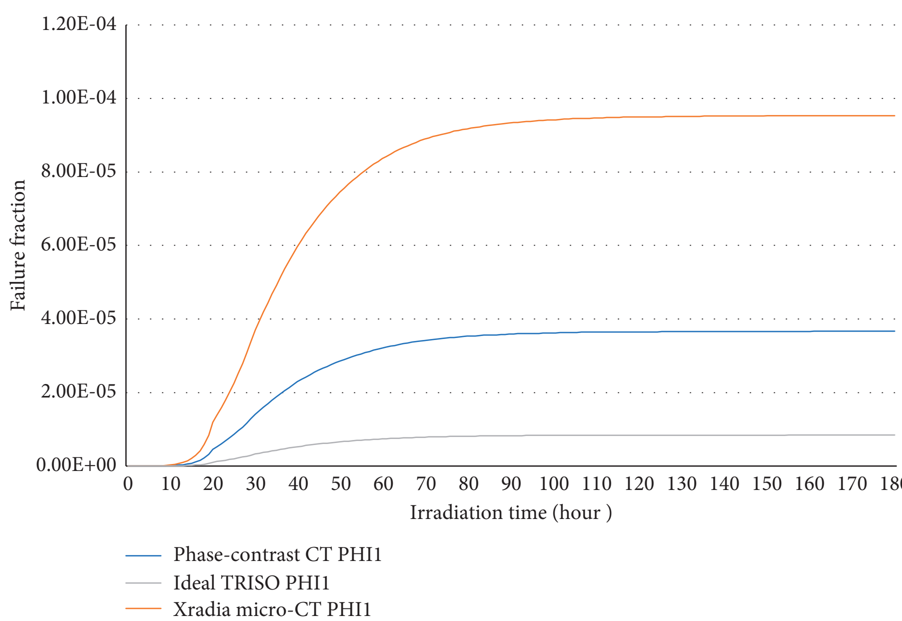

FIGURE 4: Failure fraction including corrosion versus irradiation time.

and overall failure fraction, respectively. Gas release and failure fraction increase with the irradiation time firstly and tend to be saturated.

4. Discussion

The value of overall failure fraction is almost equal to failure fraction including corrosion because failure fraction including thermal decomposition is too small compared to failure fraction including corrosion as shown in Figures 4 and 5. All failure probabilities and gas release fraction of ideal and real TRISO particle increase in first 80 hours and then go to a smoothly steady state. The increase of real TRISO grows much more rapidly than that of ideal TRISO. For the results revised with Xradia micro-CT, the release fraction of fission gas of real TRISO is 11.29 times that of ideal particle at quasi-steady state due to the increment of kernel volume. The failure fraction including corrosion of real TRISO is bigger than that of ideal TRISO, increasing by 11.29 times that of ideal particle for steady state, while the failure fraction including thermal decomposition of real TRISO is smaller than that of ideal TRISO, decreasing by 41.37% for steady state. The increase of release fraction of fission gas is similar to failure fraction including corrosion

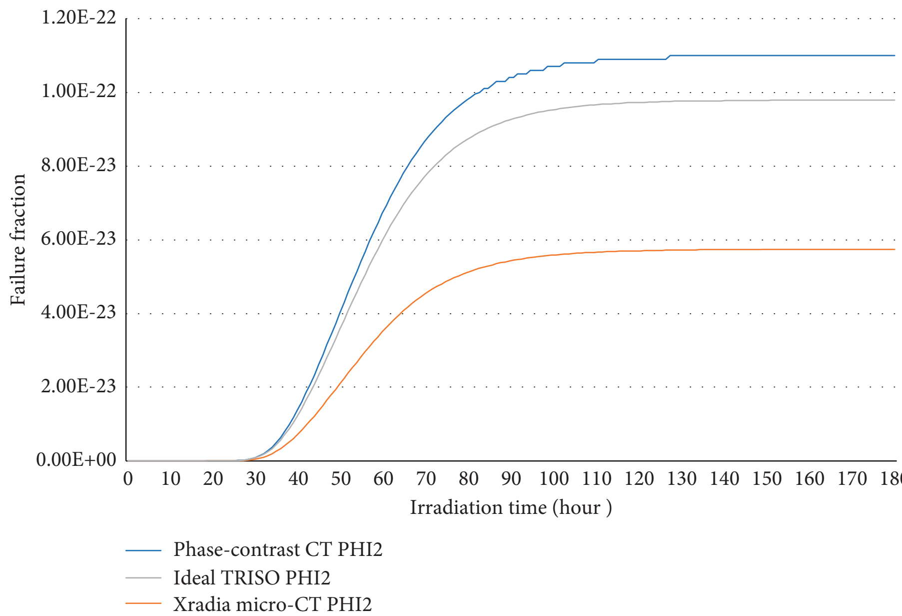

Figure 5: Failure fraction including thermal decomposition versus irradiation time.

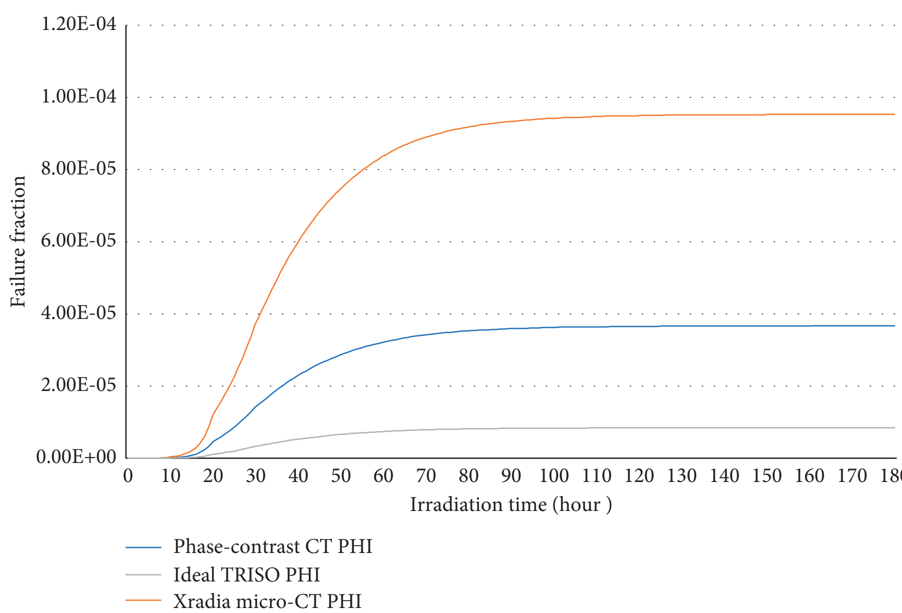

Figure 6: Overall failure fraction versus irradiation time.

because failure fraction is directly dependent on the value of stress which is proportional to the amount of fission gas release. Overall failure fraction of real TRISO increases because of the increment of kernel volume. Although the thickness of the SiC layer also increases, it can reduce failure fraction to some degree, but it is not thick enough to keep failure probability as where it was. This underlines the complexity of TRISO geometry design in terms of failure fraction. Failure fraction of thermal decomposition is dependent on the initial thickness of the SiC layer regardless of the increment of kernel volume. As the initial thickness of the SiC layer increases, the failure fraction will decrease. With respect to the results revised by synchrotron phase-contrast CT, the release fraction of fission gas and failure fraction including corrosion of measured particle are 4.35 times the ideal particle. Failure fraction including thermal decomposition of the measured particle increases by 12.36% compared with the ideal particle while overall failure fraction is 4.34 times the ideal particle at the end of the irradiation time. The failure fraction including thermal decomposition is significantly very small and almost negligible in that the calculation temperature is set in normal operation. The geometrical shape of the SiC layer has an effect on the failure fraction as the layer is the main stress holder. In PANAMA code, the SiC layer is a simplified pressure vessel with a thin shell similar to a soap bubble [9]. We are investigating a method to calculate the failure fraction with the finite element simulation of SiC stress distribution.

Total irradiation time was 180 hours, and all percentages were calculated at the end of the time. Furthermore, failure fraction is also related to irradiation temperature, and geometrical shape of kernel and the SiC layer also affect temperature distribution in TRISO. The effect of irradiation temperature on failure fraction is not discussed in this paper. The analysis and comparison in this paper is based on two particles chosen as the stochastic sample. More samples should be measured for a more comprehensive analysis.

5. Conclusions

In this paper, key geometrical parameters of real TRISO are input into PANAMA code for more accurate failure fraction calculation. Release fraction of fission gas, failure fraction including corrosion and thermal decomposition, and overall failure fraction were revised with real thickness. The fluctuation and difference of failure fraction and fission gas release fraction between real TRISO and ideal TRISO were analyzed. The stress in PANAMA for failure faction calculation can also be obtained using the finite element method by simulating the SiC layer loaded by inner pressure. In this paper, the SiC layer is assumed to be an equivalent thin wall and two particles were analyzed. Further study will be focused on the comparison between the finite element method and analytic method.

Data Availability

The data used to support the findings of this study are included within the article.

Conflicts of Interest

The authors declare that there are no conflicts of interest regarding the publication of this paper.

Acknowledgments

The authors would like to thank X-ray Imaging and Biomedical Application (BL13W1) at Shanghai Synchrotron Radiation Facility (SSRF) and University of Texas for the support of the CT experiments. The authors also want to thank Professor Bing Liu for providing surrogate TRISO particles and Professor Jianzhu Cao for providing the PANAMA code. This study was jointly supported by the National Natural Science Foundation of China (nos. 61571262, 11575095, and 61171115) and National Key Research and Development Program (no. 2016YFC0105406).

References

[1] G. K. Miller, D. A. Petti, J. T. Maki, and D. L. Knudson, "Updated solution for stresses and displacements in TRISO-coated fuel particles," *Journal of Nuclear Materials*, vol. 374, no. 1-2, pp. 129–137, 2008.

[2] G. K. Miller and J. T. Maki, "PARFUME theory and model basis report," Technical Report, Idaho National Laboratory, Idaho Falls, ID, USA, 2009.

[3] G. K. Miller, J. T. Maki, D. L. Knudson, and D. A. Petti, "Calculating failure probabilities for TRISO-coated fuel particles using an integral formulation," *Journal of Nuclear Materials*, vol. 399, no. 2-3, pp. 154–161, 2010.

[4] G. K. Miller, D. A. Petti, J. T. Maki, and D. L. Knudson, "An evaluation of the effects of SiC layer thinning on failure of TRISO-coated fuel particles," *Journal of Nuclear Materials*, vol. 355, no. 1-3, pp. 150–162, 2006.

[5] B. Cao, B. Liu, and C. H. Tang, "Stress analysis of coated particle fuel using finite element method," *Atomic Energy Science and Technology*, vol. 48, pp. 318–324, 2014.

[6] B. Liu, L. Yang, T. Liang, and C. Tang, "Stress analysis of aspherical coated particle with inner pressure," *Nuclear Engineering and Design*, vol. 251, pp. 381–384, 2012.

[7] K. Bari, C. Osarinmwian, E. López-Honorato, and T. J. Abram, "Characterization of the porosity in TRISO coated fuel particles and its effect on the relative thermal diffusivity," *Nuclear Engineering and Design*, vol. 265, pp. 668–674, 2013.

[8] T. Lowe, R. S. Bradley, S. Yue et al., "Microstructural analysis of TRISO particles using multi-scale X-ray computed tomography," *Journal of Nuclear Materials*, vol. 461, pp. 29–36, 2015.

[9] K. Verfondern, "TRISO fuel performance modeling and simulation," *Comprehensive Nuclear Materials*, vol. 3, pp. 755–788, 2012.

[10] R. Gontard and H. Nabielek, "Performance evaluation of modern HTR TRISO fuels," KFA Report HTA-IB-05/90, Technical Report, Forschungszentrum Jülich GmbH, Jülich, Germany, 1990.

[11] Y.-W. Lee, J.-Y. Park, Y. K. Kim et al., "Development of HTGR-coated particle fuel technology in Korea," *Nuclear Engineering and Design*, vol. 238, no. 11, pp. 2842–2853, 2008.

[12] F. Montgomery, "Fission product SiC reaction in HTGR fuel," Technical Report GA-905837, General Atomics, San Diego, CA, USA, 1981.

[13] L. Zhu, U. Ewert, X. Xiang, Y. Peng, and X. Wang, "Synchrotron phase-contrast CT to segment the structure boundaries of a TRISO-coated particle," *NDT & E International*, vol. 103, pp. 12–18, 2019.

[14] L. B. Zhu, X. C. Xiang, Y. H. Peng, and X. Wang, "Three dimensional measurement of TRISO-coated particle using micro computed tomography," *Science and Technology of Nuclear Installations*, Article ID 2908538, 8 pages, 2019.

[15] https://www.vsg3d.com.